



Outline

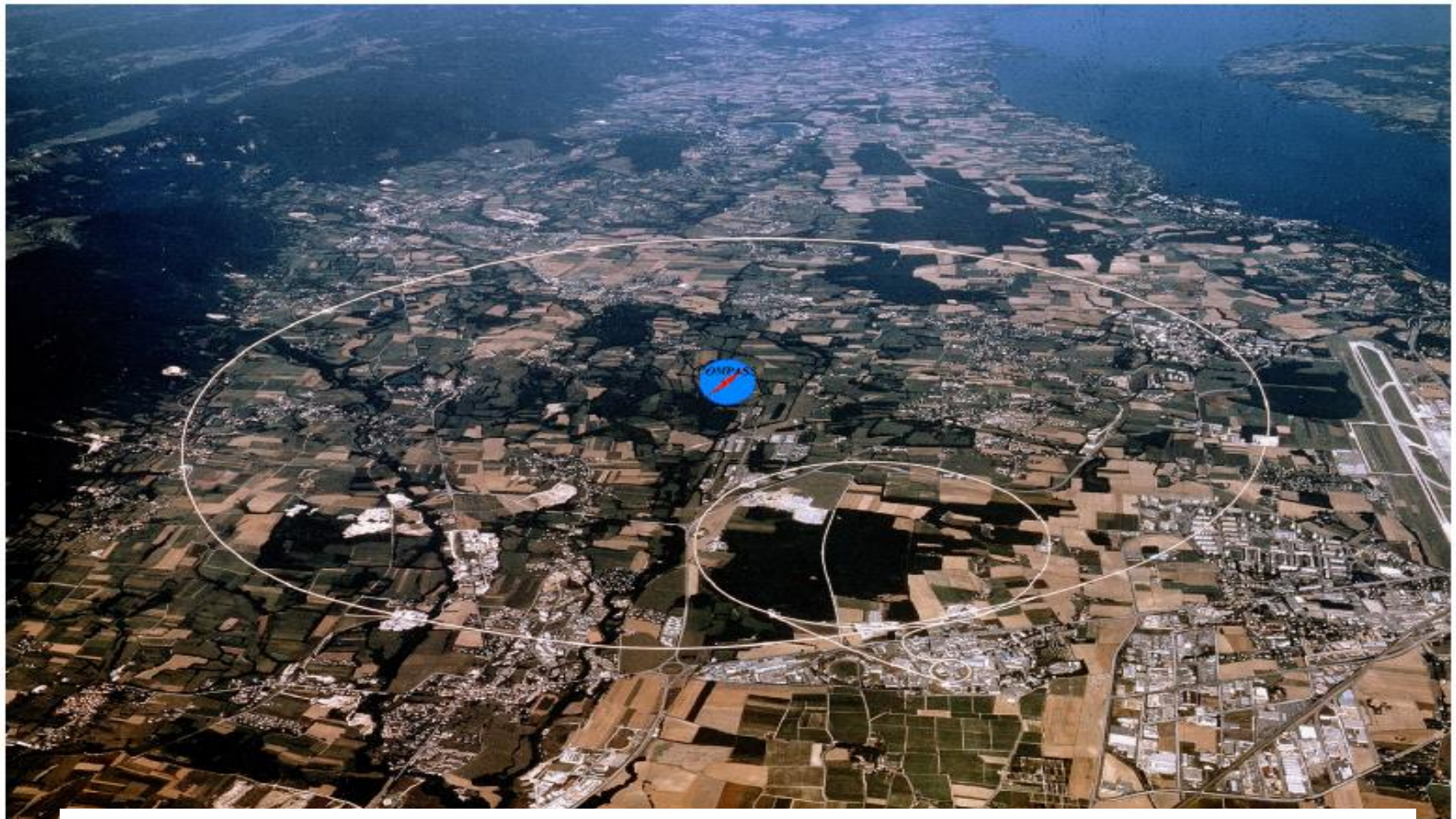


- 1. Hadron structure and excited states**
 - Light quark spectroscopy - update
 - Pion polarizability and ChPT applicability test
- 2. Nucleon structure with muon beam**
 - Multiplicities
 - Azimuthal asymmetries transverse/longitudinal
- 3. DVCS and DVMP**
 - DVCS – 2016+2017
- 4. Dell-Yan**
 - 2015+2018 data set
- 5. Proton radius Beam test**
- 6. 2021 deuteron run**
- 7. Summary**

Only selected topics were addressed in the talk, see COMPASS annual report for detailed info.

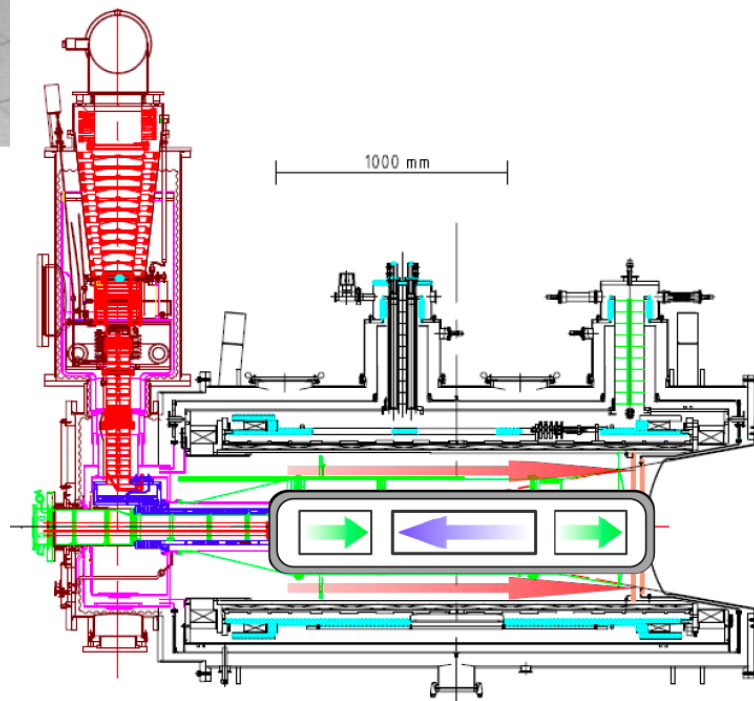
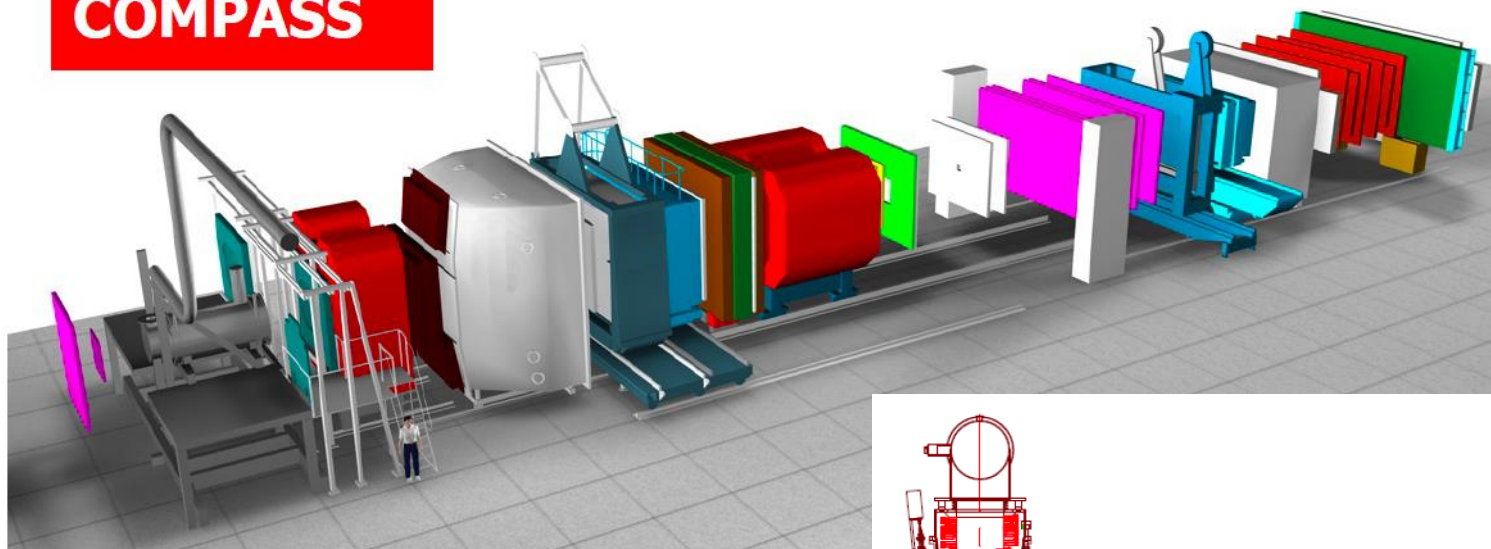
COMPASS QCD facility at CERN (SPS)

COmmon Muon Proton Apparatus for Structure and Spectroscopy



~210 physicists, 12 countries + CERN, 24 institutions

COMPASS



Universal and flexible apparatus.

Most important features of the two-stage COMPASS Spectrometer:

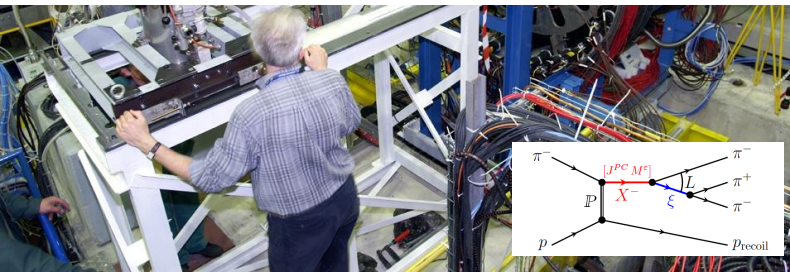
1. Muon, electron or hadron beams with the momentum range 20-250 GeV and intensities up to 10^8 particles per second
2. Solid state polarised targets (NH_3 or ${}^6\text{LiD}$) as well as liquid hydrogen target and nuclear targets
3. Powerful tracking (350 planes) and PiD systems (Muon Walls, Calorimeters, RICH)



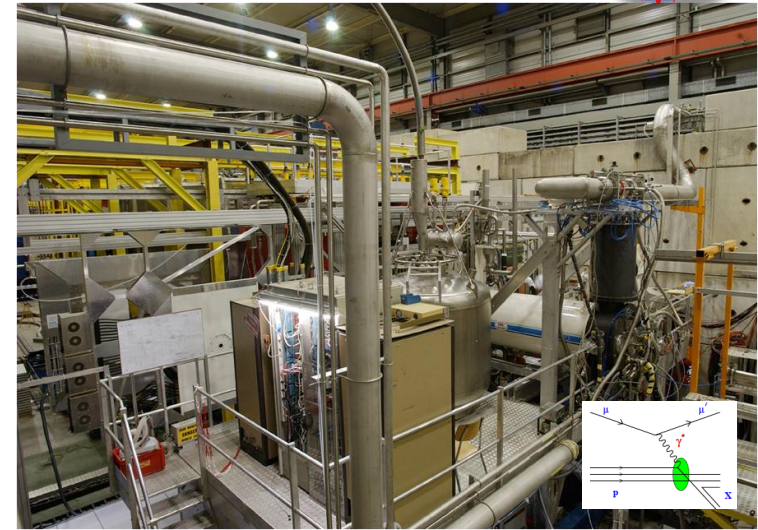
COMPASS QCD facility at SPS M2 beam line (CERN) (secondary hadron and lepton beams)



Exotic states, chiral dynamics



**COMPASS-I
1997-2011**



Polarised SIDIS

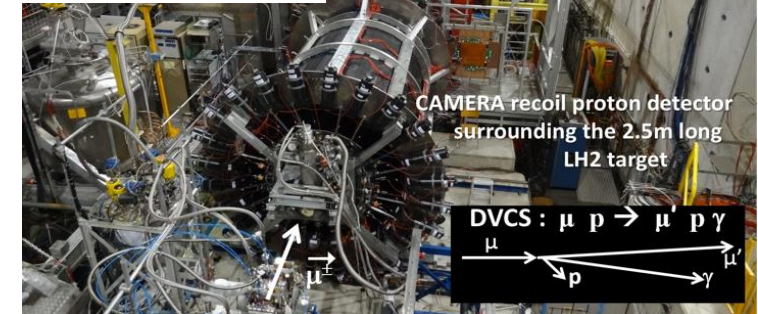
Hadron Spectroscopy & Polarisability

**3D hadron structure, ↗
Proton spin decomposition
↘ (spin crisis) ↘**

**COMPASS-II
2012-2020**

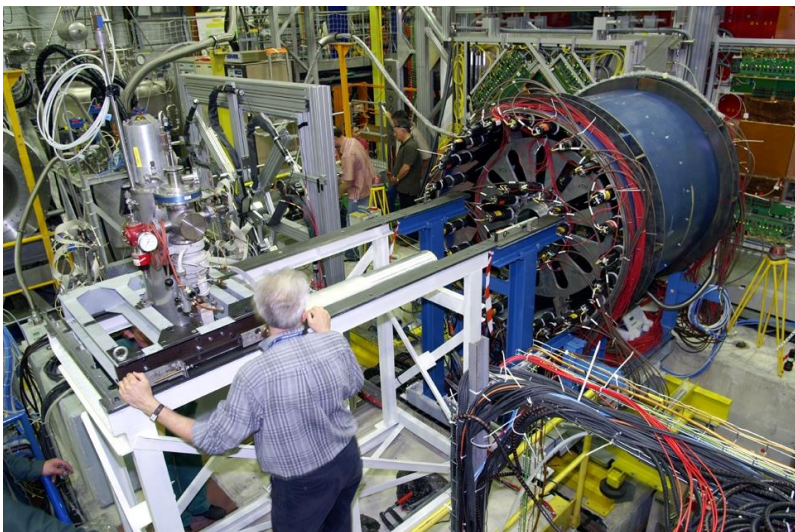


Polarised Drell-Yan



CAMERA recoil proton detector surrounding the 2.5m long LH2 target

DVCS (GPDs) + unp. SIDIS



2008-2009 data taking, 190 GeV/c hadron beam on a hydrogen target.

3π data sample $\sim 50 \times 10^6$ exclusive events – factor 10 to 100 to previous experiment

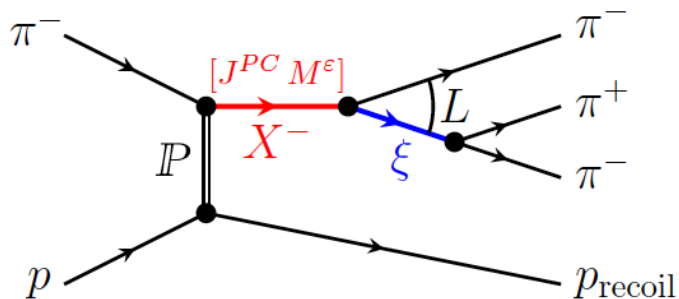
Potential illustration – discovery of a new resonance-like $a_1(1420)$ state in $1^{++}0^+ f_0(980)\pi$ P wave (PRL).

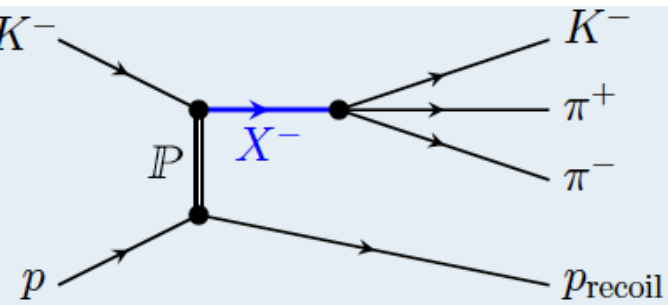
A lot of work has been invested to develop new methods in order to cope with huge data sample.
A lot of work has been invested to develop new methods in order to cope with huge data sample.

An extensive papers that describes the PWA method and the results from this analysis has recently been published ([PRD 95 \(2017\) 032004](#), [PRD 98 \(2018\) 092003](#)). Major step forward in the field: 100 bins in $m_{3\pi}$ (0.5 to 2.5 GeV/c²) and 11 in t' (0.1 to 1.0 (GeV/c)²), 88 waves up to spin 6.

Analysis steps:

1. p-w decomposition: 88x88 spin-density matrix for each t' (f.-m. transfer squared) and $m_{3\pi}$ bin (mass-independent fit)
2. For selected wave set (14 waves, 60% of total intensity) fit of the spin-density matrix by a resonance models (B.-W. + coherent non-resonant term)

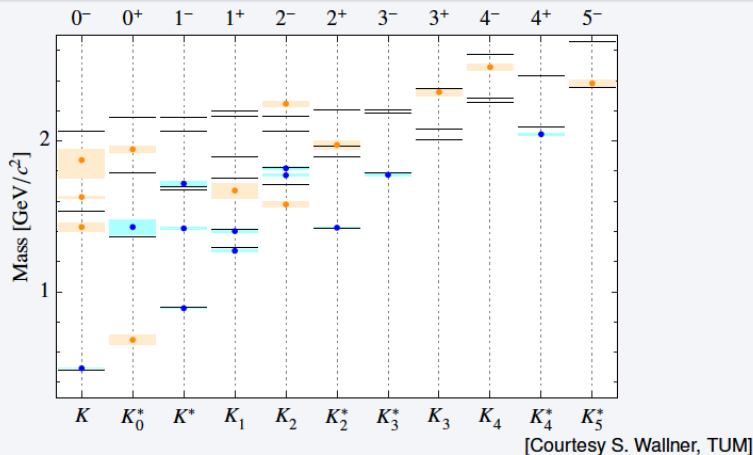




In 2008 and 2009 runs, we obtain about 728 000 exclusive $K^- \pi^- \pi^+$ events (x4 compare to WA03). The analysis is more complicated compare to 3π final state as non only $\pi^- \pi^+$ but also $K^- \pi^+$ isobars. Currently we use 6 isobars to analyse $\pi\pi$ final states and another 6 to $K\pi$. We use 4 t' bins and 20 to 40 MeV/c^2 mass bins in the range 0-3 GeV/c^2 . Clear signal from dominant states was observed

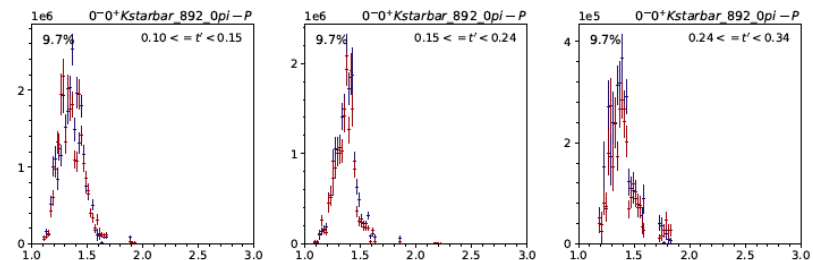
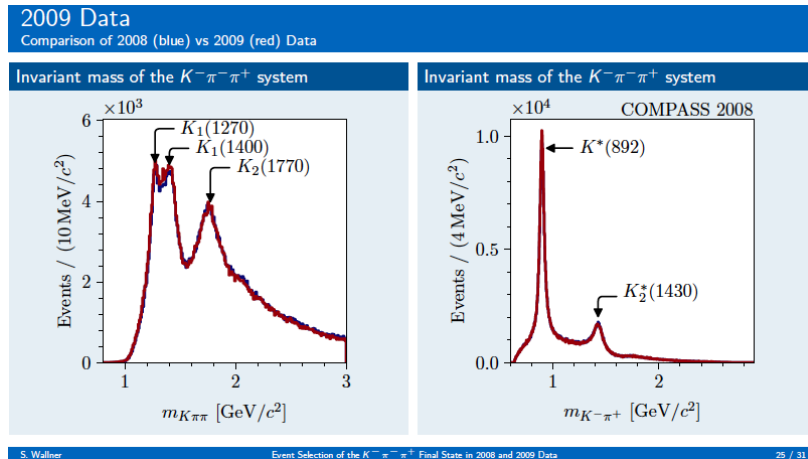
PDG 2016: 25 kaon states below $3.1 \text{ GeV}/c^2$

- Only 12 kaon states in summary table, 13 need confirmation
- Many predicted quark-model states still missing
- Some hints for supernumerous states



Boris Grube, TU München

Hadron Spectroscopy with Kaon Beam





Diffraction dissociation III

new results on odd-spin waves + work in progress



Joint effort with JPAC

In collaboration with **Joint Physics Analysis Center (JPAC)** $\eta(\prime) \pi^-$ final state analysis as odd-spin waves have spin-exotic quantum number. More refined with respect to the simple Breit-Wigner approach analysis of the P- and D-waves in $\eta \pi^-$ and $\eta' \pi^-$ final states shows that only one resonance pole consistent with spin exotic $\pi_1(1600)$ is necessary to describe both waves (no need for two close in mass spin-exotic states $\pi_1(1600)$ and $\pi_1(1400)$).

WORK in Progress: Because of the huge data set a special effort has to be taken to reduce systematic uncertainties and to refine analysis model/method.

1. Choice of parametrization for the $\pi^+ \pi^-$ isobar amplitude
2. Another source of systematic uncertainties is a truncation of the partial-wave expansion. We have developed a method which permit automatically define the wave set depending on mass of 3π system.



Measurement of chiral dynamics in the reaction $\pi^- \gamma^* \rightarrow \pi^- \pi^0$

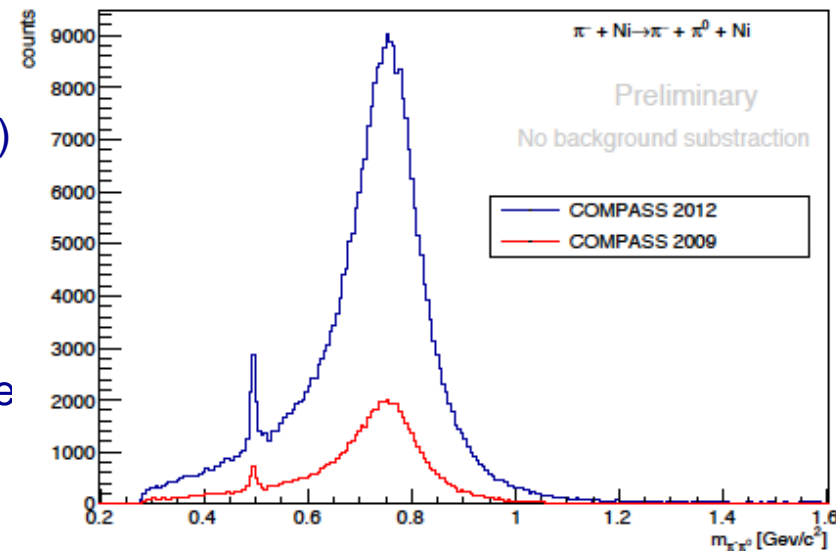


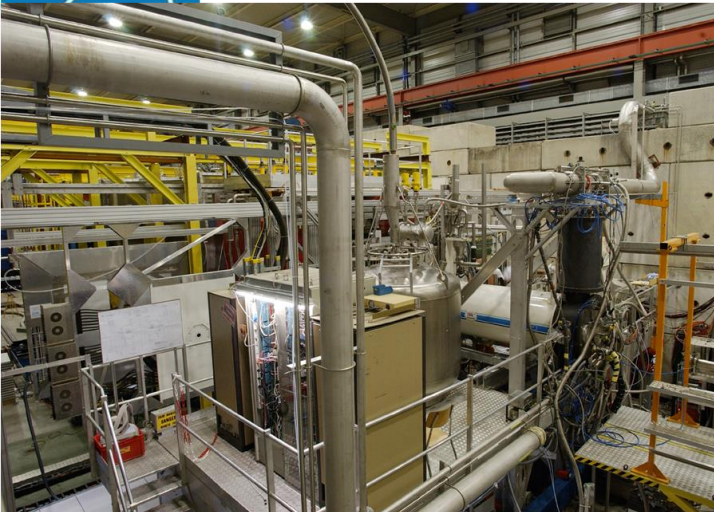
Data taking periods in 2009 and 2012, we concentrate on $\pi^- \gamma^* \rightarrow \pi^- \pi^0$ (other final states like $\pi^- \gamma^* \rightarrow \pi^- \gamma$, $\pi^- \gamma^* \rightarrow \pi^- \pi^+ \pi^-$, $\pi^- \gamma^* \rightarrow \pi^- \pi^0 \pi^0$ are available) in order to study chiral anomaly $F_{3\pi}$.

$\pi^- \pi^0$ final state is dominated by $\rho(770)$ resonance. Previous experiments that measured $F_{3\pi}$ to 10% level were restricted to the threshold mass region because of the low mass tail of the ρ , with limited control over systematic.

New in our analysis:

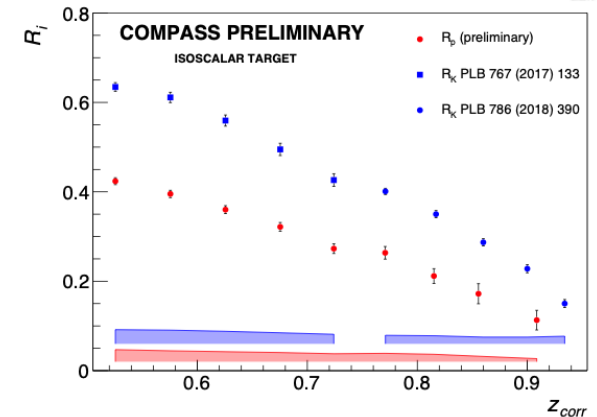
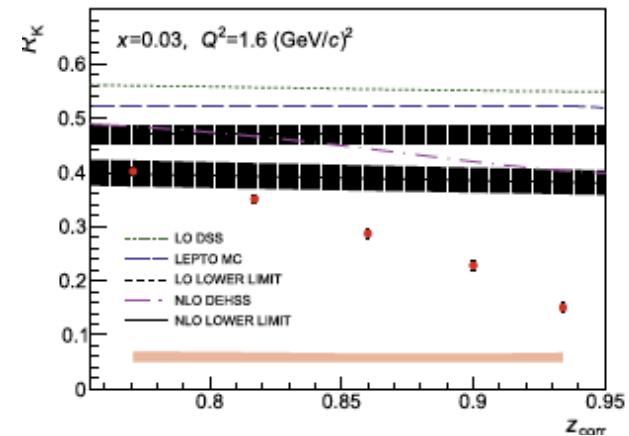
- Analysis of the $\pi^- \pi^0$ mass spectrum in **Hoferichter approach** (extension of the ChPT amplitude up to $\sim 1 \text{ GeV}/c^2$ by including $\rho(770)$ via dispersion relation) in a much wider mass range \rightarrow precise $F_{3\pi}$ measurement + ρ radiative coupling extraction;
- New method to control the integrated luminosity via K^- decay channel in $\pi^- \pi^0$ and $\pi^- \pi^0 \pi^0$. Both channels Gives now compatible results (after detailed study of the Acceptance corrections in MC)





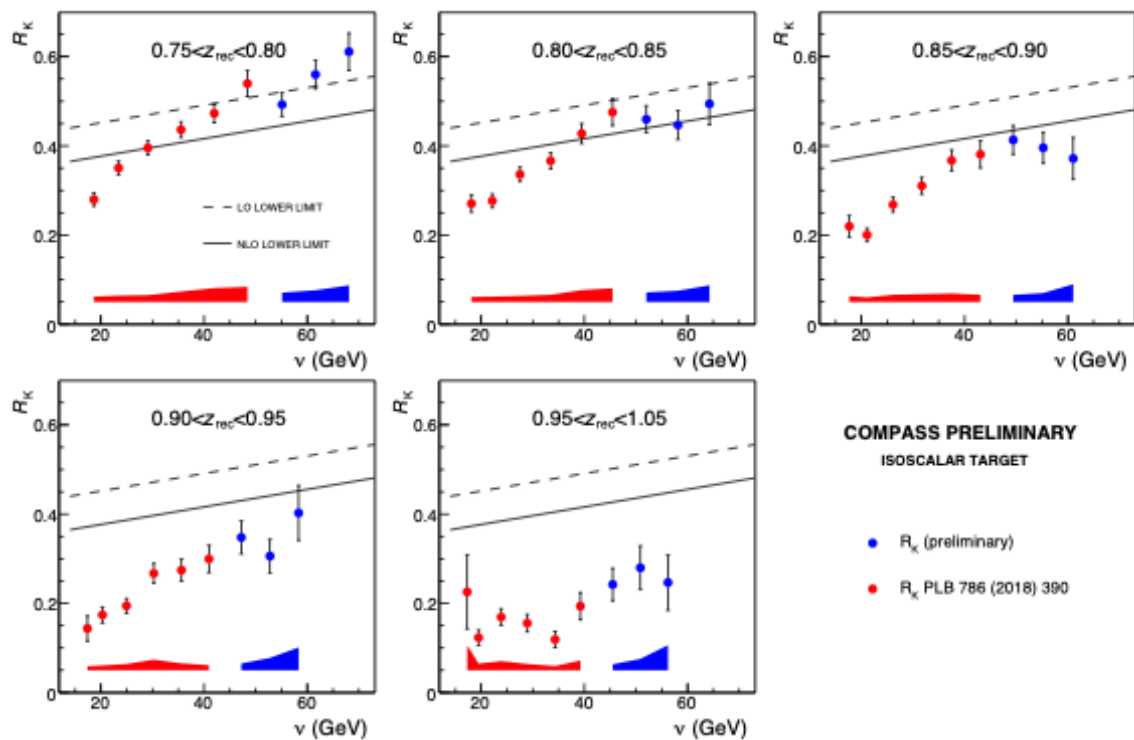
In the last report we summarised our studies of K^-/K^+ multiplicity ratio R_K in the region of high z , ($z > 0.75$) ([PLB 786 \(2018\) 390](#)). The obtained results were below the lower limit obtained from LO and NLO pQCD calculations. The discrepancy between measured R_K and lower limit expected from pQCD was increasing with z and reached a factor 2.5 for the highest measured z value, about 0.93.

Kaon multiplicities ratio shows also strong dependence on the M_{missing} of the process, so remaining phase space has to be taking into account.



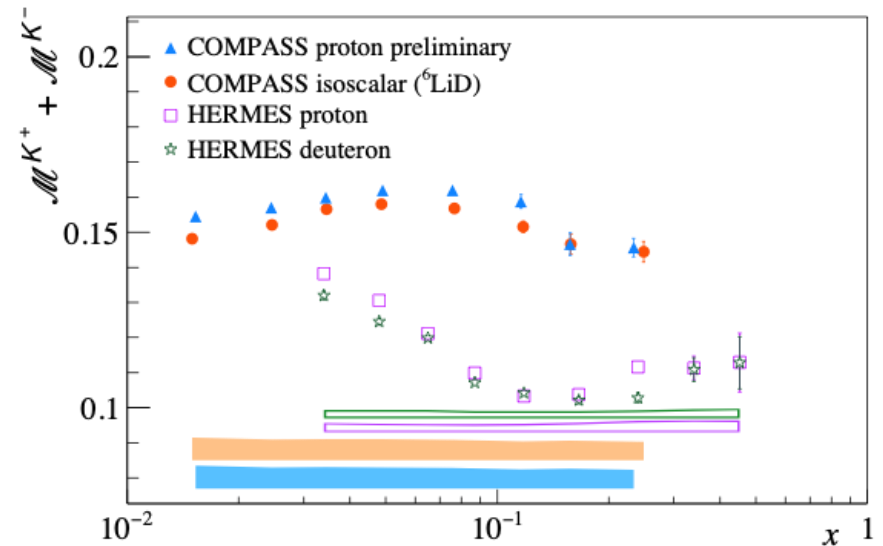
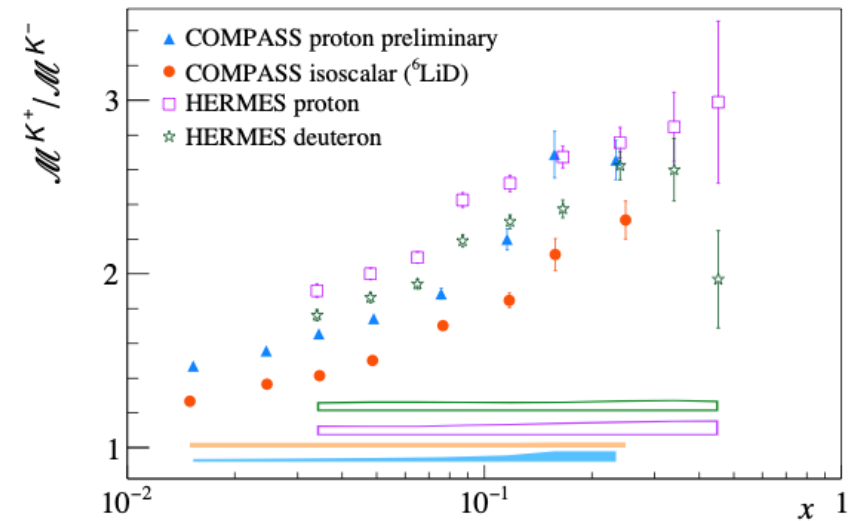
Using our 2006 data set we have continued our multiplicities study for protons and antiprotons by extracting the $p\bar{p}/p$ multiplicity ratio R_p for $z > 0.5$. We have found that in the whole measured phase space the ratio is below the lower limit allowed by LO pQCD of about 0.5. Note that the discrepancy to the LO QCD prediction is much larger in the proton case than for kaons.

Over the past year the range of \sqrt{s} has been extended by increasing hadron momentum range (better K separation at high momenta (NN technique)). Additional points were added for each Z bin studied before. Sort of saturation effect could be noticed.



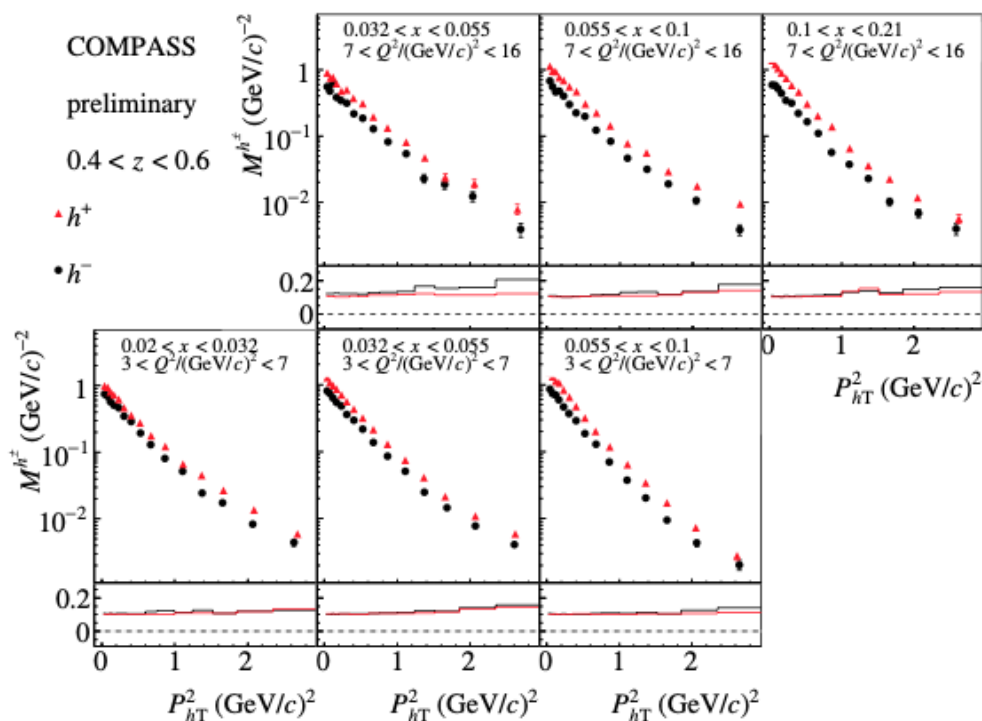
We have started 2016 data analysis (LH² target) in order to extract kaon multiplicities on proton target. As a first step we have extracted R_K in the same bins as for the iso-scalar target data (integrating over z and averaging over y). It is expected that proton R_K is 10-20% higher compared to isoscalar.

Important message – HERMES and COMPASS data are still in tension.
 Can not be explained only by different Q^2 range, the discussion is going on.



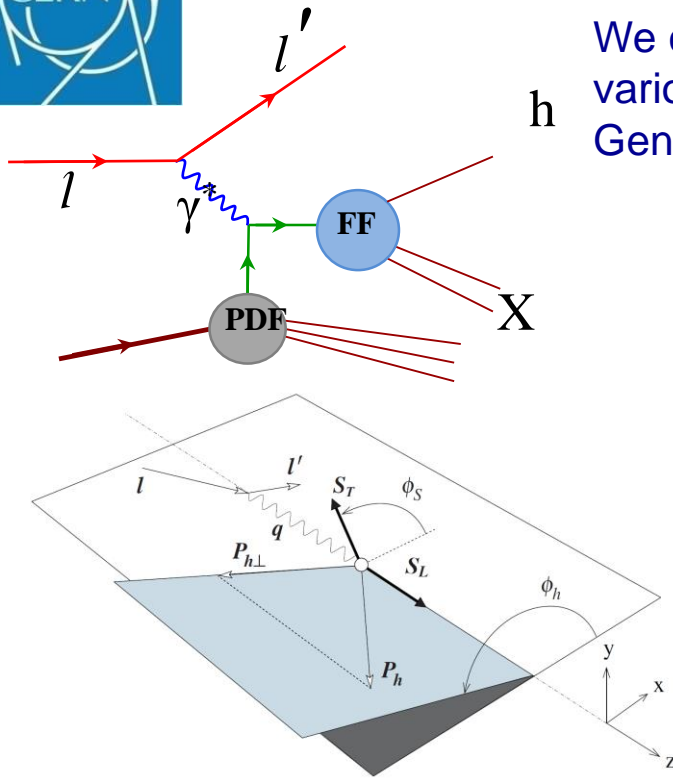
Another multiplicity related activity: extraction from our 2016 proton data P_T dependent multiplicities. As a first step we use the same kinematical (x , Q^2 , z) bins as for the deuteron data.

Released data corresponds to the range where the acceptance corrections to P_T distributions $< 30\%$. Shown results corresponds to $< 1/10$ of all available statistics.



We continue to scrutinize polarised SIDIS data by studying various target spin-dependent azimuthal asymmetries.

General expression for SIDIS cross-section in terms of asymmetries



$$\frac{d\sigma}{dx dy dz d(p_T^h)^2 d\phi_h d\psi} = 2 \left[\frac{\alpha}{xyQ^2} \frac{y^2}{2(1-\varepsilon)} \left(1 + \frac{\gamma^2}{2x} \right) \right] (F_{UU,T} + \varepsilon F_{UU,L})$$

$$\times \left\{ 1 + \sqrt{2\varepsilon(1+\varepsilon)} A_{UU}^{\cos\phi_h} \cos\phi_h + \varepsilon A_{UU}^{\cos(2\phi_h)} \cos(2\phi_h) + \lambda \sqrt{2\varepsilon(1-\varepsilon)} A_{LU}^{\sin\phi_h} \sin\phi_h \right.$$

$$+ S_L \left[\sqrt{2\varepsilon(1+\varepsilon)} A_{UL}^{\sin\phi_h} \sin\phi_h + \varepsilon A_{UL}^{\sin(2\phi_h)} \sin(2\phi_h) \right]$$

$$+ S_L \lambda \left[\sqrt{1-\varepsilon^2} A_{LL} + \sqrt{2\varepsilon(1-\varepsilon)} A_{LL}^{\cos\phi_h} \cos\phi_h \right]$$

$$+ S_T \left[A_{UT}^{\sin(\phi_h-\phi_S)} \sin(\phi_h-\phi_S) + \varepsilon A_{UT}^{\sin(\phi_h+\phi_S)} \sin(\phi_h+\phi_S) + \varepsilon A_{UT}^{\sin(3\phi_h-\phi_S)} \sin(3\phi_h-\phi_S) \right.$$

$$\left. + \sqrt{2\varepsilon(1+\varepsilon)} A_{UT}^{\sin\phi_S} \sin\phi_S + \sqrt{2\varepsilon(1-\varepsilon)} A_{UT}^{\sin(2\phi_h-\phi_S)} \sin(2\phi_h-\phi_S) \right]$$

$$+ S_T \lambda \left[\sqrt{(1-\varepsilon^2)} A_{LT}^{\cos(\phi_h-\phi_S)} \cos(\phi_h-\phi_S) \right.$$

$$\left. + \sqrt{2\varepsilon(1-\varepsilon)} A_{LT}^{\cos\phi_S} \cos\phi_S + \sqrt{2\varepsilon(1-\varepsilon)} A_{LT}^{\cos(2\phi_h-\phi_S)} \cos(2\phi_h-\phi_S) \right] \left. \right\},$$

LO LSA/TSA	twist-2: PDF \otimes FF
$A_{UL}^{\sin(2\phi_h)}$	$h_{1L}^{\perp q} \otimes H_{1q}^{\perp h}$
A_{LL}	$g_{1L}^q \otimes D_{1q}^h$
$A_{UT}^{\sin(\phi_h-\phi_S)}$	$f_{1T}^{\perp q} \otimes D_{1q}^h$
$A_{UT}^{\sin(\phi_h+\phi_S-\pi)}$	$h_1^q \otimes H_{1q}^{\perp h}$
$A_{UT}^{\sin(3\phi_h-\phi_S)}$	$h_{1T}^{\perp q} \otimes H_{1q}^{\perp h}$
$A_{LT}^{\cos(\phi_h-\phi_S)}$	$g_{1T}^q \otimes D_{1q}^h$

subleading LSA/TSA	higher-twist PDF \otimes FF	WWA twist-2: PDF \otimes FF
$A_{UL}^{\sin(\phi_h)}$	$xh_L^q \otimes H_{1q}^{\perp h}, xf_L^{\perp q} \otimes D_{1q}^h$	$h_{1L}^{\perp q} \otimes H_{1q}^{\perp h}$
$A_{LL}^{\cos(\phi_h)}$	$xe_L^q \otimes H_{1q}^{\perp h}, xg_L^{\perp q} \otimes D_{1q}^h$	$g_{1L}^q \otimes D_{1q}^h$
$A_{UT}^{\sin(\phi_S)}$	$xf_T^q \otimes D_{1q}^h, xh_T^q \otimes H_{1q}^{\perp h}, xh_T^{\perp q} \otimes H_{1q}^{\perp h}$	$f_{1T}^{\perp q} \otimes D_{1q}^h, h_1^q \otimes H_{1q}^{\perp h}$
$A_{UT}^{\sin(2\phi_h-\phi_S)}$	$xf_T^{\perp q} \otimes D_{1q}^h, xh_T^q \otimes H_{1q}^{\perp h}, xh_T^{\perp q} \otimes H_{1q}^{\perp h}$	$f_{1T}^{\perp q} \otimes D_{1q}^h, h_1^q \otimes H_{1q}^{\perp h}$
$A_{LT}^{\cos(\phi_S)}$	$xg_T^q \otimes D_{1q}^h, xe_T^q \otimes H_{1q}^{\perp h}, xe_T^{\perp q} \otimes H_{1q}^{\perp h}$	$g_{1T}^q \otimes D_{1q}^h$
$A_{LT}^{\cos(2\phi_h-\phi_S)}$	$xg_T^{\perp q} \otimes D_{1q}^h, xe_T^q \otimes H_{1q}^{\perp h}, xe_T^{\perp q} \otimes H_{1q}^{\perp h}$	$g_{1T}^q \otimes D_{1q}^h$

New approach - weighted asymmetries

Asymmetries obtained by weighting the spin-dependent part of the cross-section with powers of p_T^h .

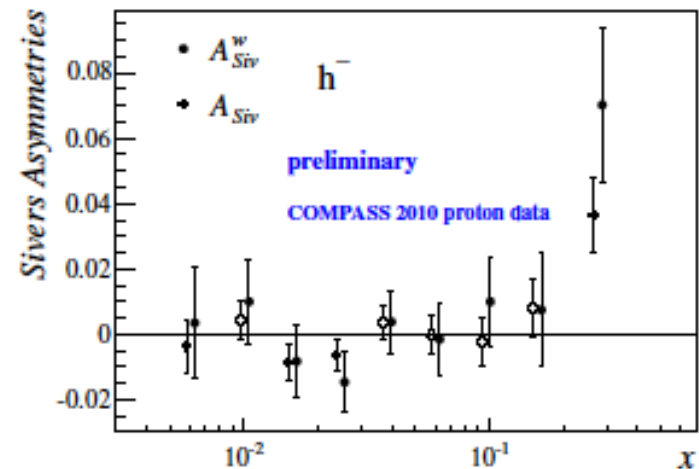
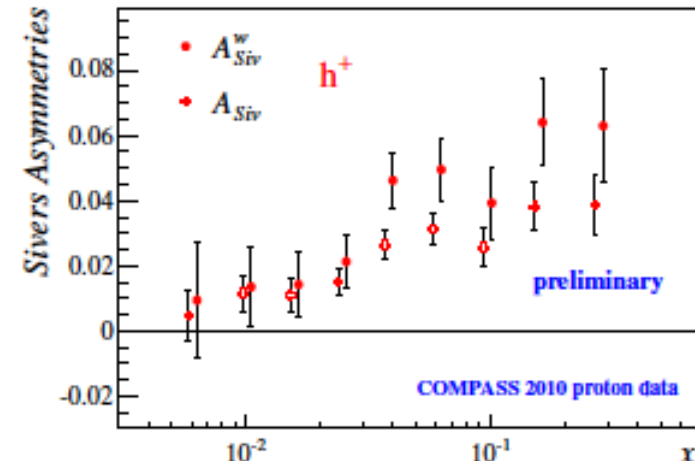
Main advantage - convolution integrals becomes products → no parametrization of the unknown transverse momentum dependence of PDFs and FFs is needed..

$$A_{Siv}^{(p_T^h/zM)}(x, z) = 2 \frac{\sum_q e_q^2 f_{1T}^{\perp(1)q}(x) \cdot D_1^q(z)}{\sum_q e_q^2 f_1^q(x) \cdot D_1^q(z)},$$

Important: large statistics, good acceptance.

Allows to extract first moment of Sivers

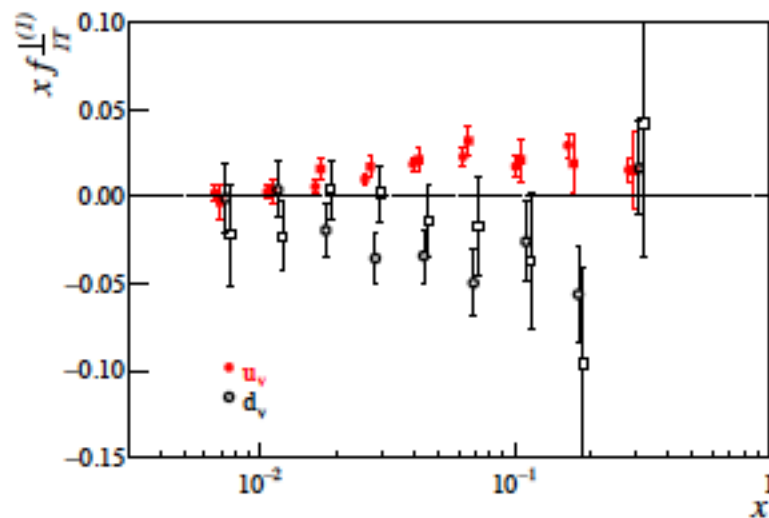
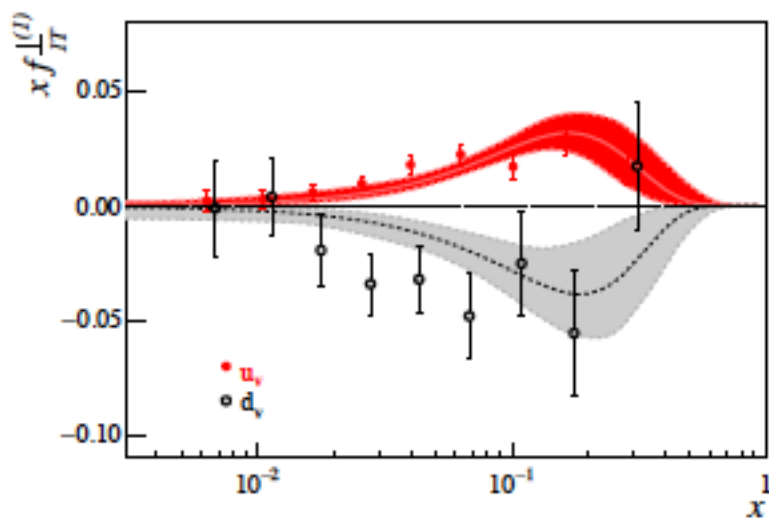
$$f_{1T}^{\perp(1)}(x, Q^2) = \int d^2 k_T \frac{k_T^2}{2M^2} f_{1T}^{\perp}(x, k_T, Q^2).$$



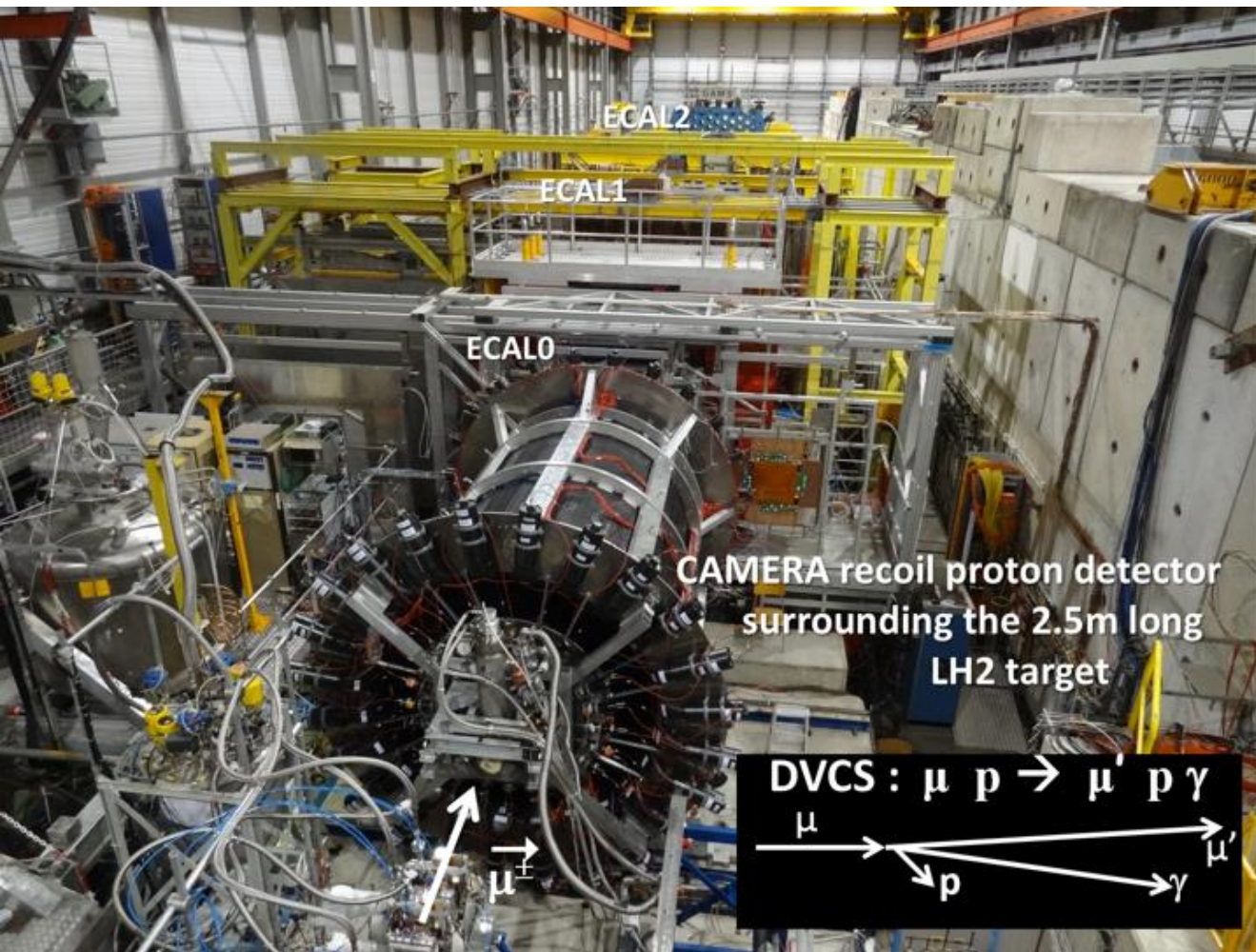
This is a first data on p_T^h weighted Sivers asymmetry

New approach - weighted asymmetries

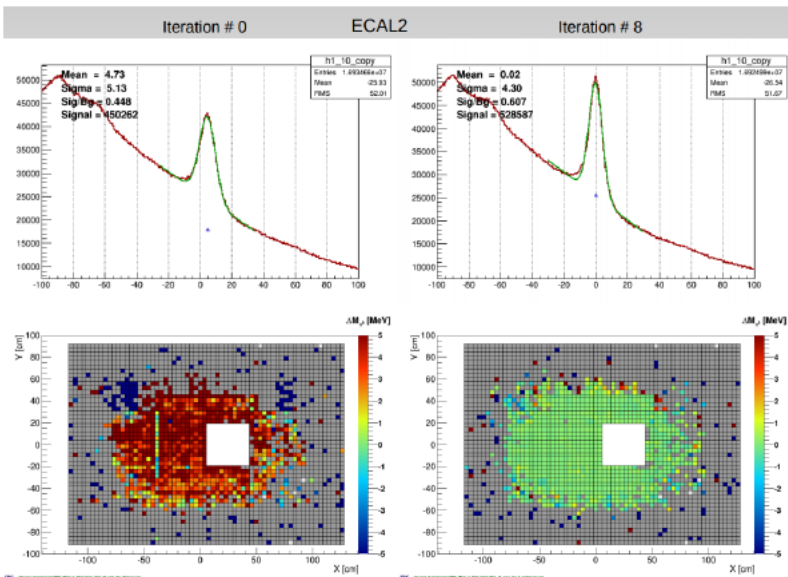
The measurement of the Sivers asymmetries weighted with the hadron transverse momentum in the N system P_T , was already described in the previous report. Also, the first moments of the Sivers functions for the u_v and d_v quarks could be extracted in each x bin from the P_T/zM -weighted Sivers asymmetries with no assumptions on the transverse momentum dependence of PDFs and FFs. Because of the lack of deuteron data the Sivers function for the sea quarks had to be assumed vanish. The first moments of the Sivers functions are shown in fig. 23, together with previous extractions from d and p data. As can be seen the agreement is good. This is an important fact, since the Sivers function is a recently introduced PDF, and its knowledge is still scarce: the agreement among extractions which use different methods strengthen the robustness of the result.



(first DVCS results were reported last year)



2016-17, 160 GeV pion beam for calibration, μ^+ and μ^- for physics, 2.5 meters long LH₂ target



In 2016 and 2017 we were taking data with Approximately the same mu+ and mu- beam Intensities in order to avoid normalization Problems faced during 2012 DVCS pilot run.

Significant time were spent to calibrate Ecals And Proton Recoil Detector. Data looks fine now.

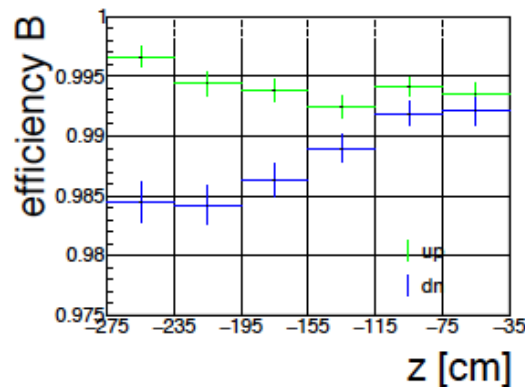
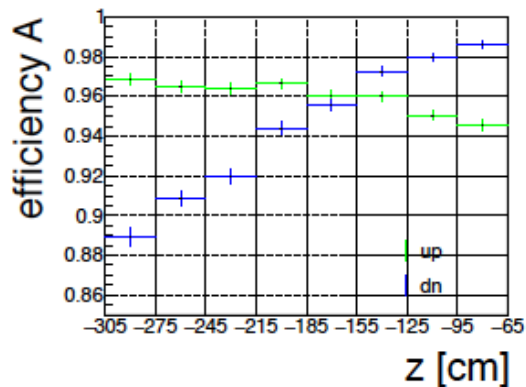
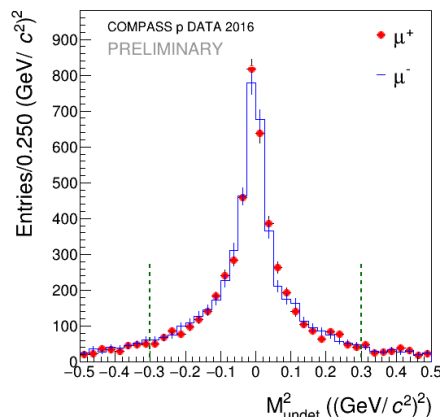
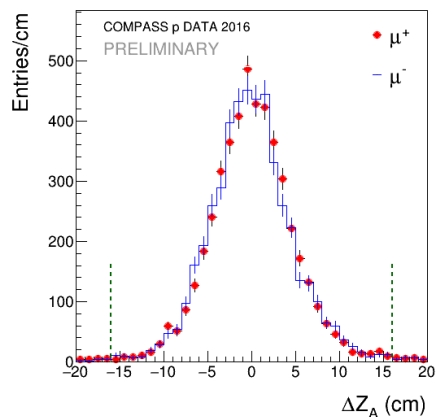
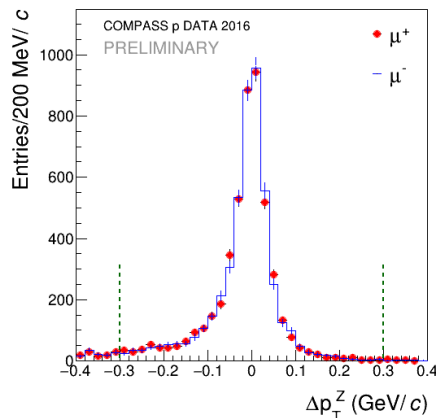
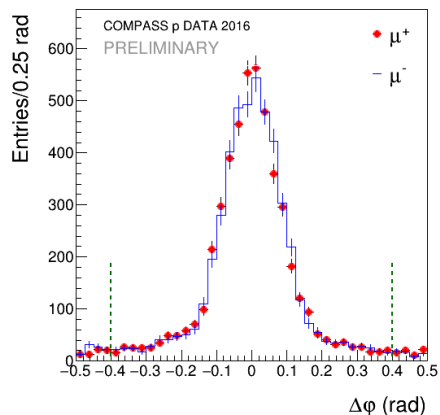


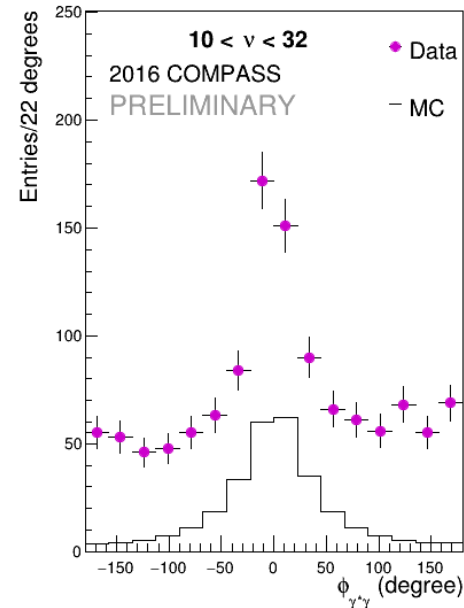
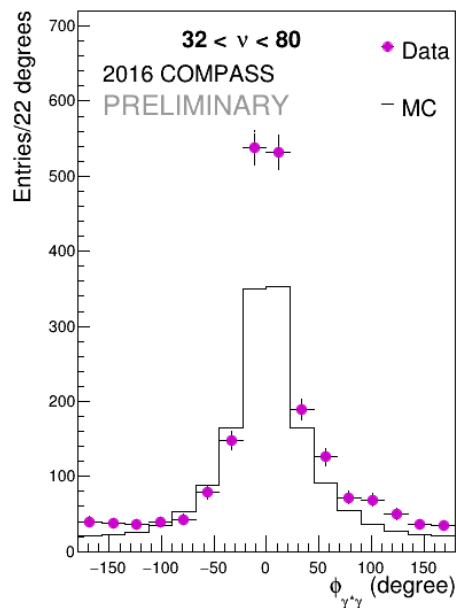
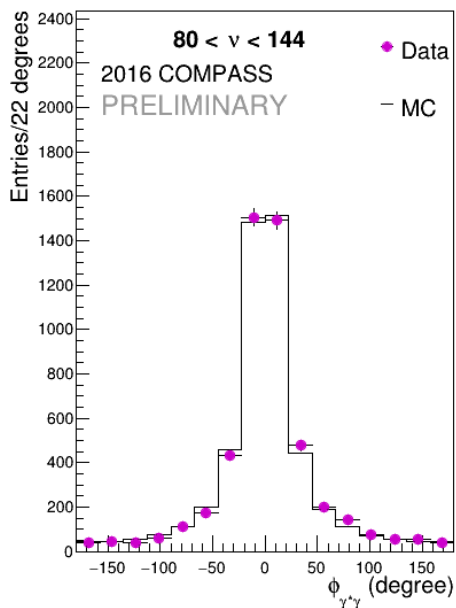
Fig. 13: Average efficiencies of all up- and downstream PMTs vs. the z position in the scintillators in the kinematic range $0.08 (\text{GeV}/c)^2 \leq t \leq 0.64 (\text{GeV}/c)^2$.

Mu+/mu- normalisation issue is not there any more in exclusive reaction $\mu p \rightarrow \mu' p' \gamma$



All distribution obtained with mu- beam was normalised to the same luminosity (or the same number of muons) for which distributions for mu+ beam were obtained. At variance to 2012 DVCS pilot run (~10-15% difference) pilot run we see very good agreement.

At the very preliminary stage of this analysis we can present the exclusive single photon events obtained as a function of $\phi_{\gamma^*\gamma}$ for the sum of the mu+ and mu- beam contributions in 3 ranges (as for the 2012 results). The data are compared to the BH MC prediction normalized to the bin at large $\phi_{\gamma^*\gamma}$ ($80 < \sqrt{s} < 144$ GeV).



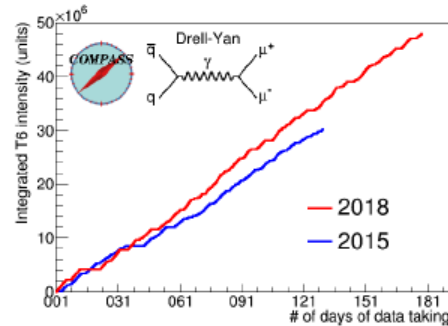
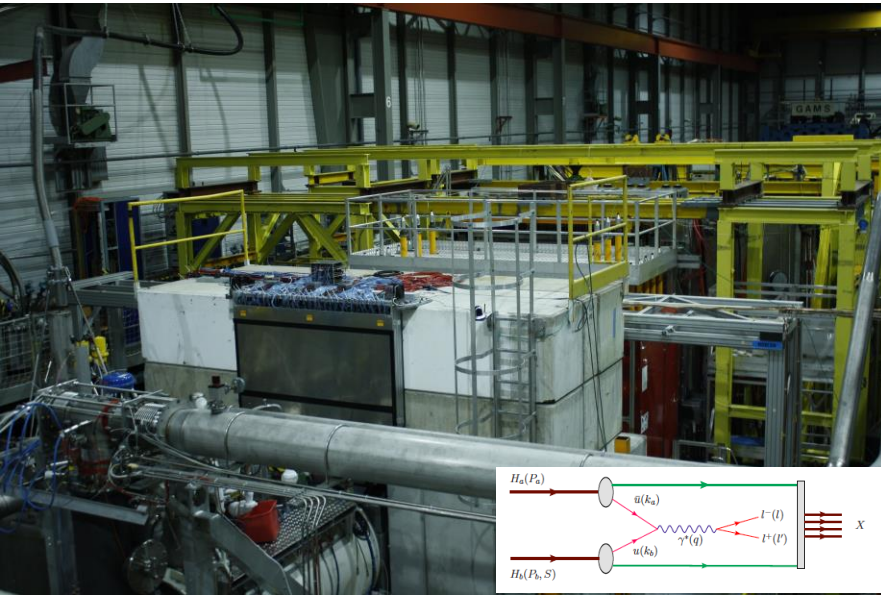


Table 2: Average polarisation in transverse mode for the four spin state configuration during 2018 and 2015 Drell-Yan runs.

Year	upstream cell		downstream cell	
	↑	↓	↑	↓
2018	75.5%	-69.8%	72.4%	-68.4%
2015	74.2%	-71.4%	69.2%	-67.0%

2015:

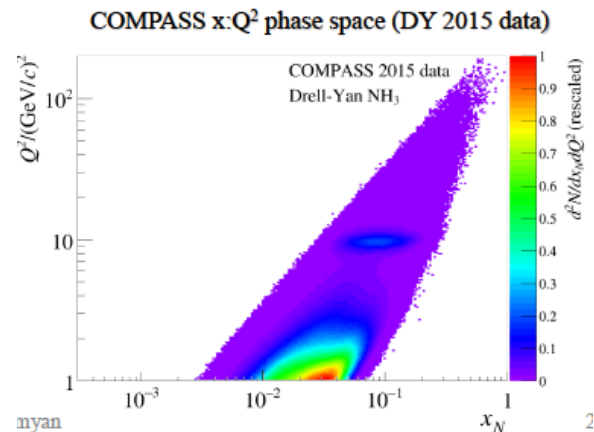
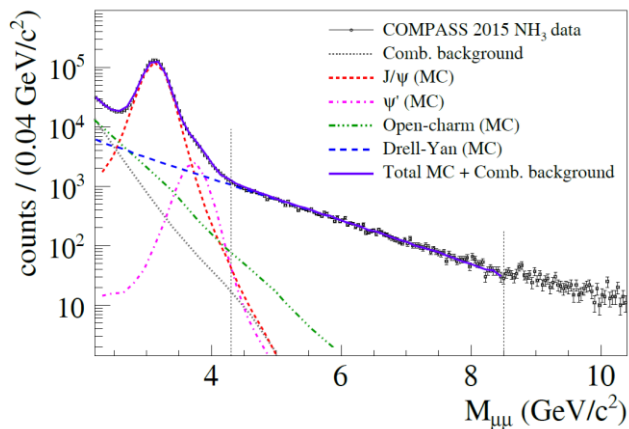
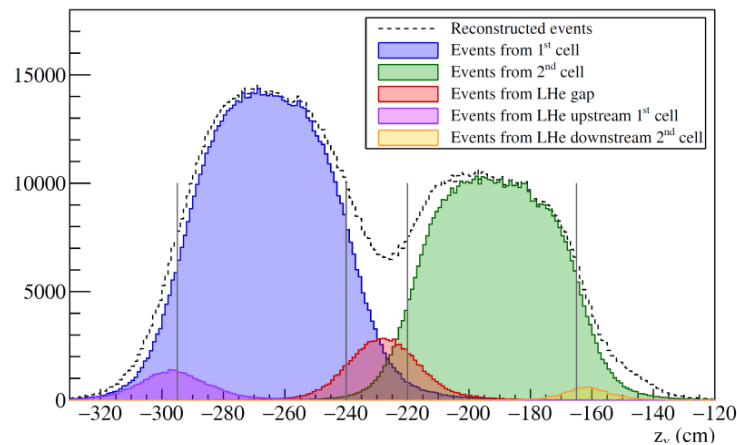
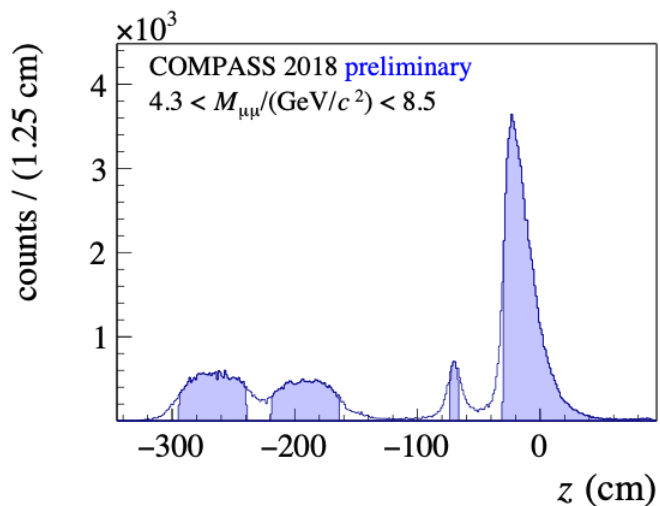
Good machine performance: on average 84%

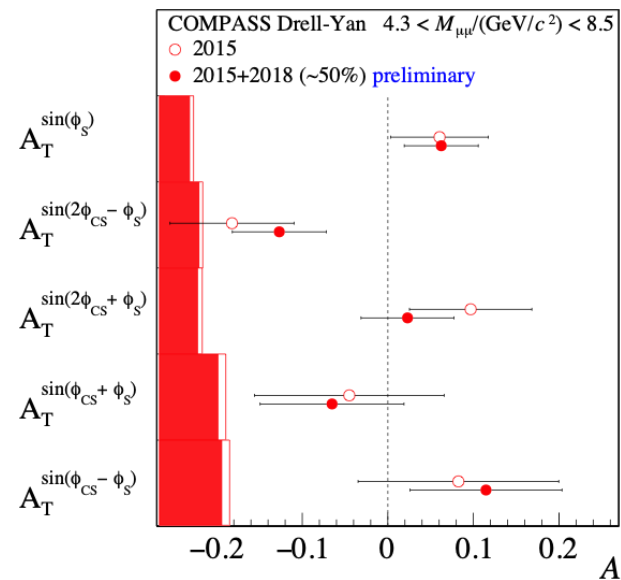
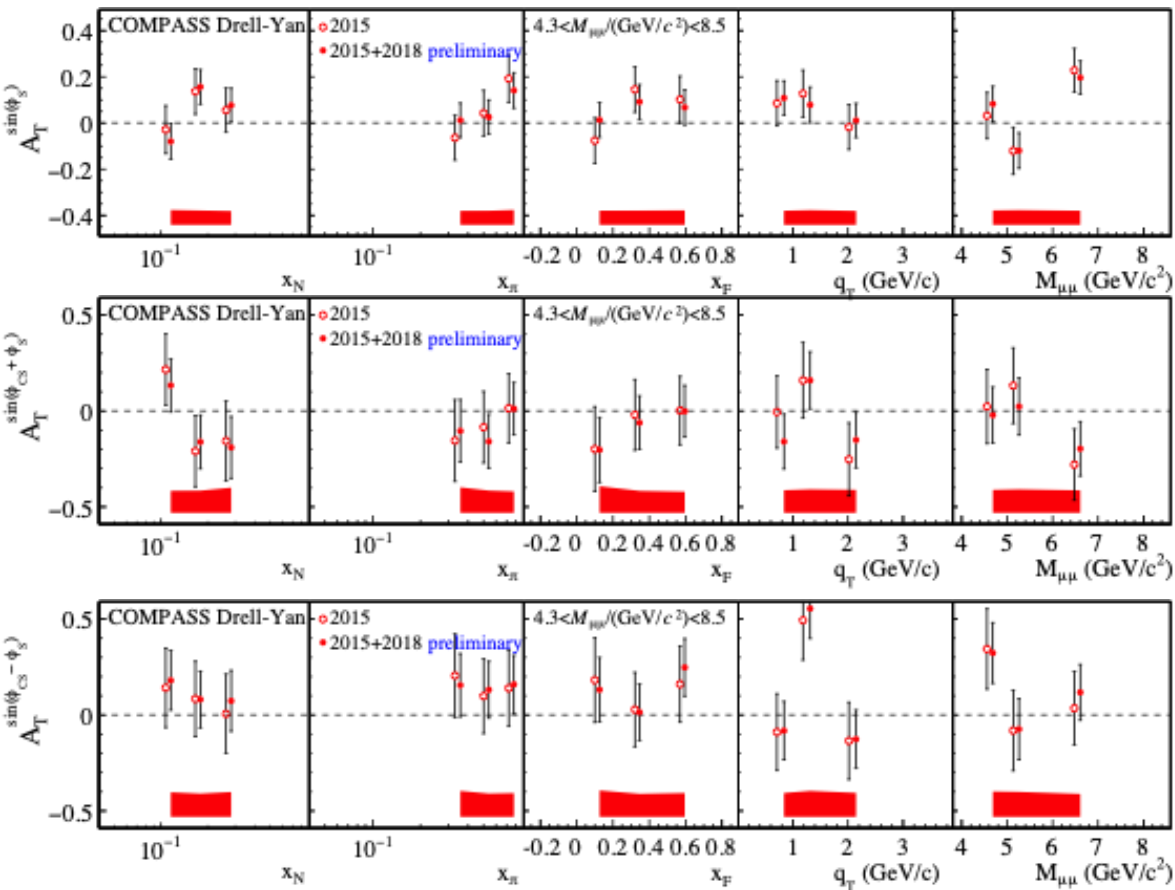
Good spectrometer availability: ~80%

2018:

Poor machine performance: ~ 74%

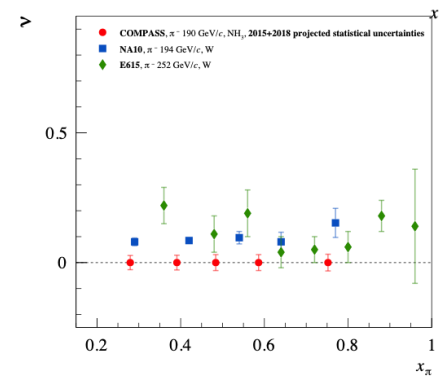
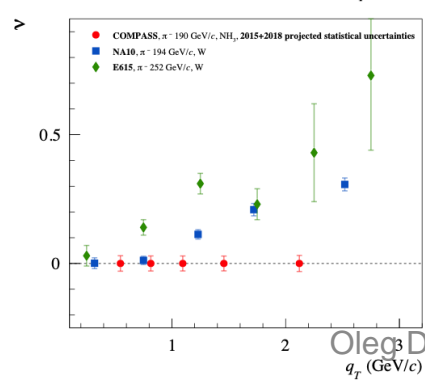
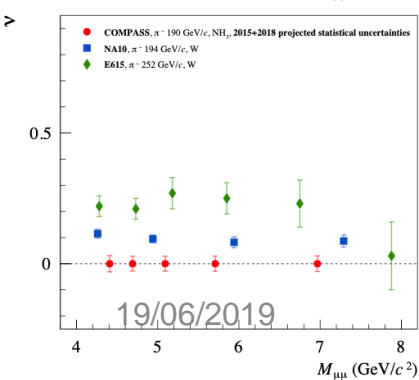
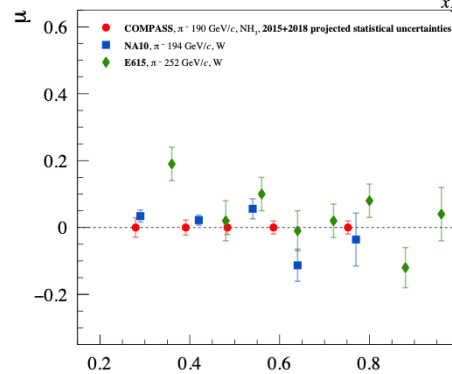
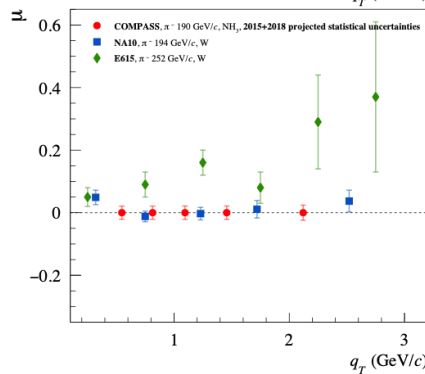
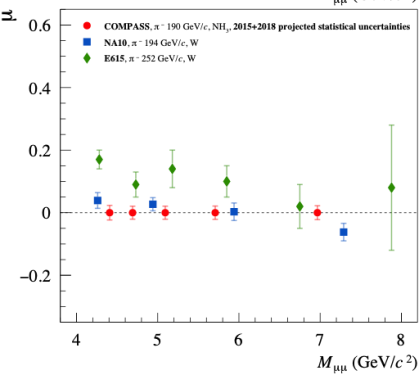
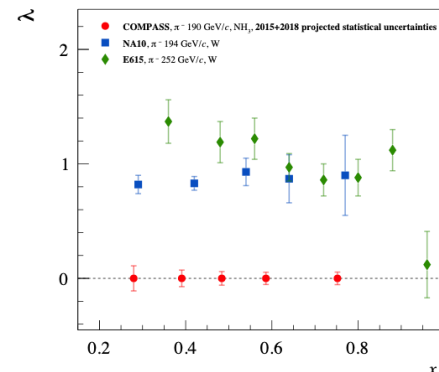
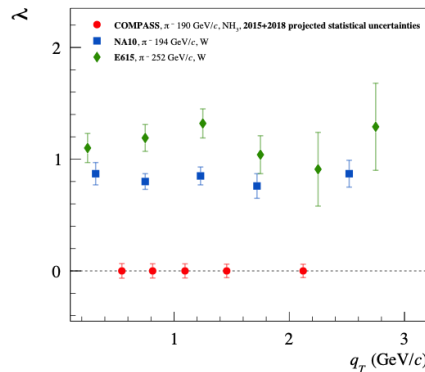
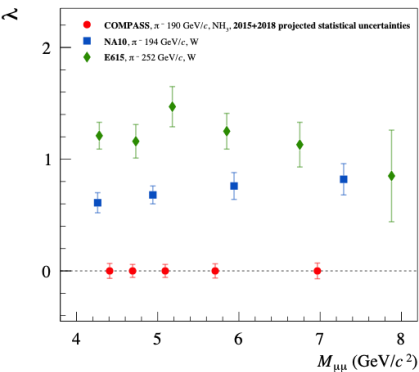
Lower compared to 2015 spectrometer efficiency: ~74 %





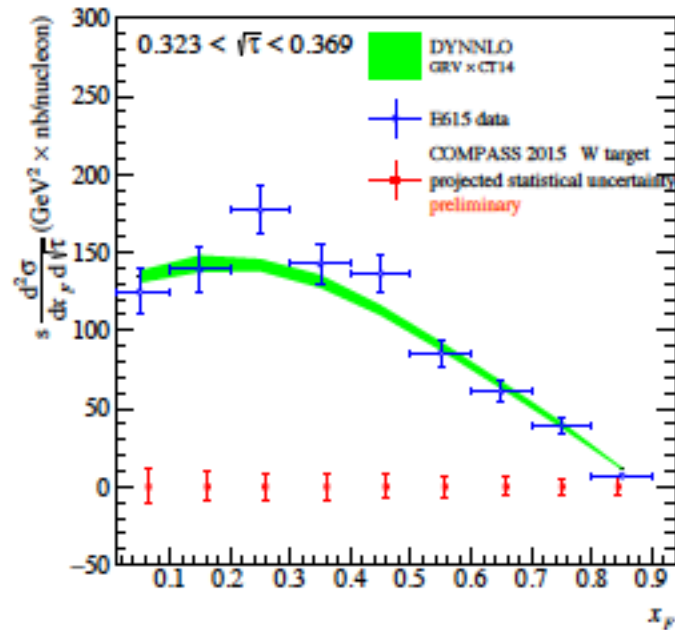
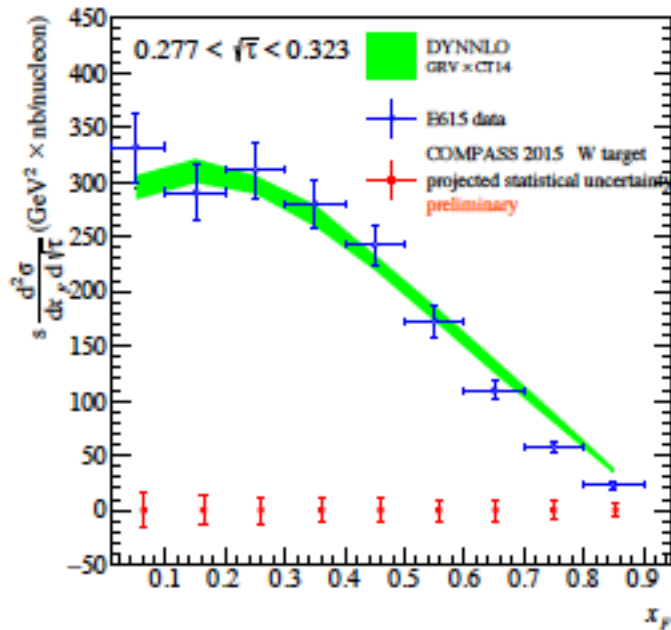
COMPASS-II preliminary
2015 + 50% 2018 results

$$\frac{1}{\sigma} \frac{d\sigma}{d\Omega} = \frac{3}{4\pi} \frac{1}{\lambda+3} \left(1 + \lambda \cos^2 \theta + \mu \sin^2 \theta \cos \phi + \frac{\nu}{2} \sin^2 \theta \cos 2\phi \right)$$



19/06/2019

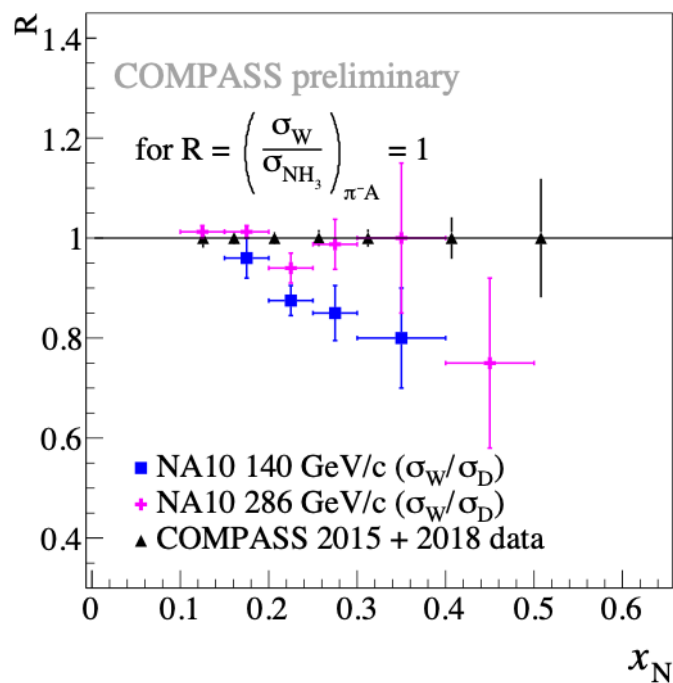
COMPASS-II DY absolute cross-sections, work in progress, below projections for 2015 (W) compared to E615



COMPASS-II DY – nuclear effects (EMC)

The ratio $R_{\pi-A}$ of the Drell-Yan cross-sections per nucleon for the NH_3 and W targets of COMPASS corrected for the difference in number of protons and neutrons, can be expressed as

$$R_{\pi-A} = \frac{\sigma_W}{\sigma_{\text{NH}_3}} = \frac{\mathcal{L}_{\text{NH}_3}}{\mathcal{L}_W} k_{pm} \frac{N_{\mu\mu}^W \text{Acc}^{\text{NH}_3}}{N_{\mu\mu} \text{Acc}^W} = C \frac{N_{\mu\mu}^W}{N_{\mu\mu}^{\text{NH}_3}} \quad (8)$$



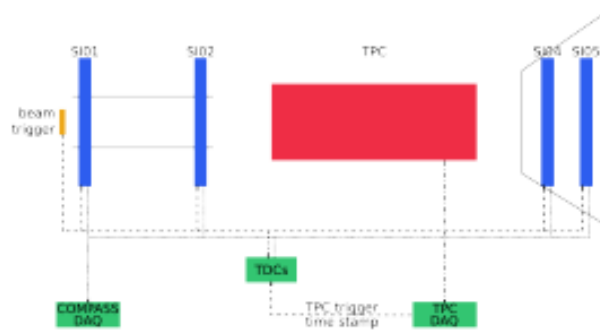
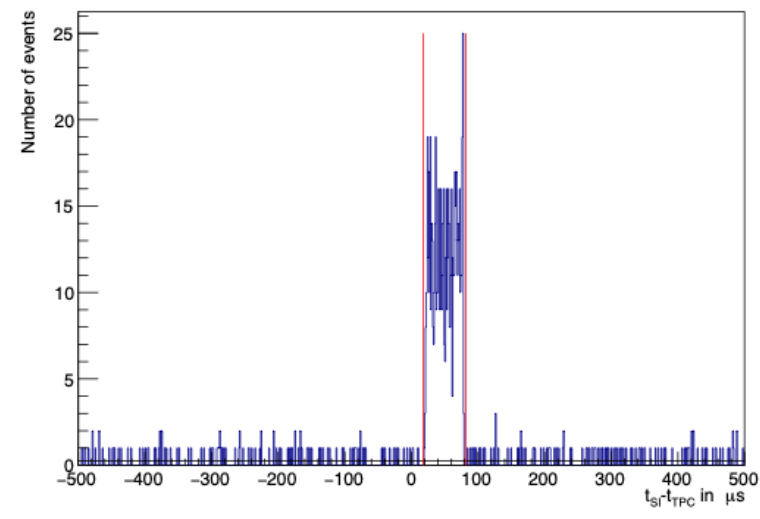
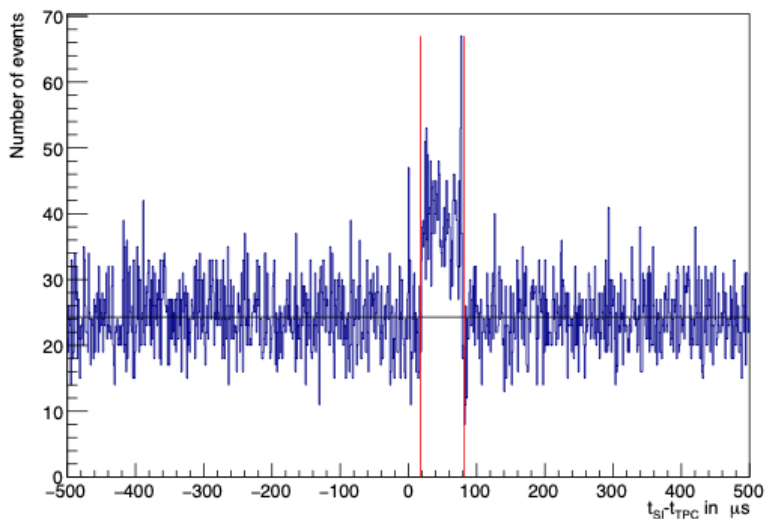


Fig. 50

Time difference

Time difference



Theta \geq 0.2 mrad and radial cuts

additional cuts on the z-coordinate and that the central pads of the TPC anode are hit

Masters thesis, Martin Hoffmann, Helmholtz-Institut für Strahlen- und Kernphysik, Universität Bonn

One year of data taking with muon beam and transversely polarized deuteron target was Approved by CERN RB in June 2018 (150 days of running).

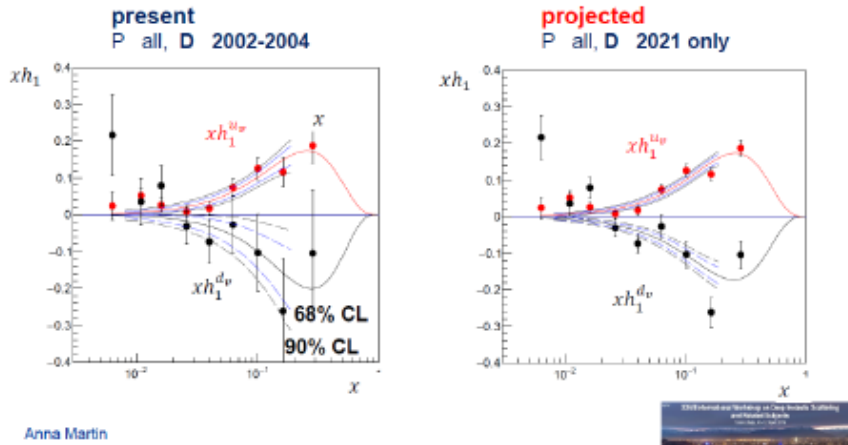
Motivation: COMPASS has very unbalance data set on TP targets: deuteron data set is almost order of magnitude smaller compared to proton. In order to extract flavour separated

TMDs, Transversity and to constrain tensor charge one has to have approximately equal

new deuteron data: impact for the tensor charge

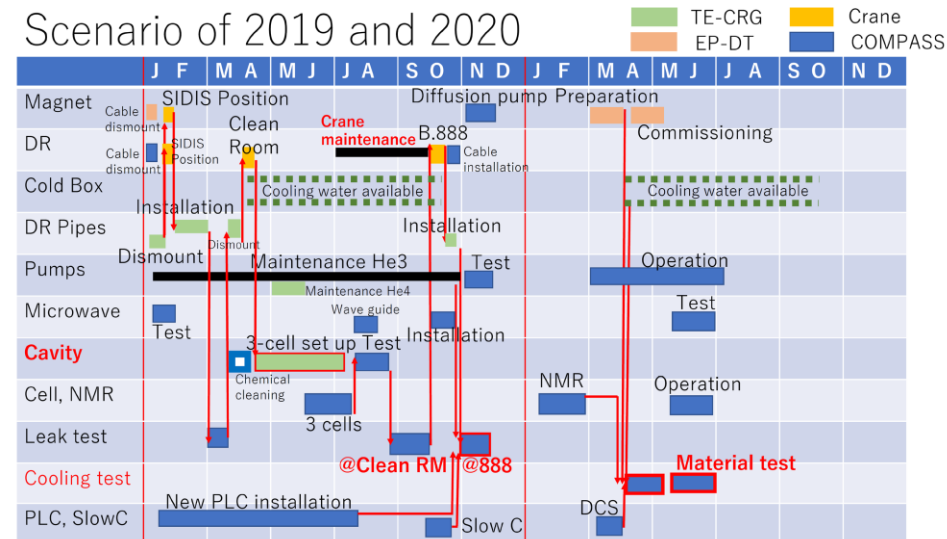
using all the existing proton data
COMPASS 2010 and 2007 plus HERMES ("P all")

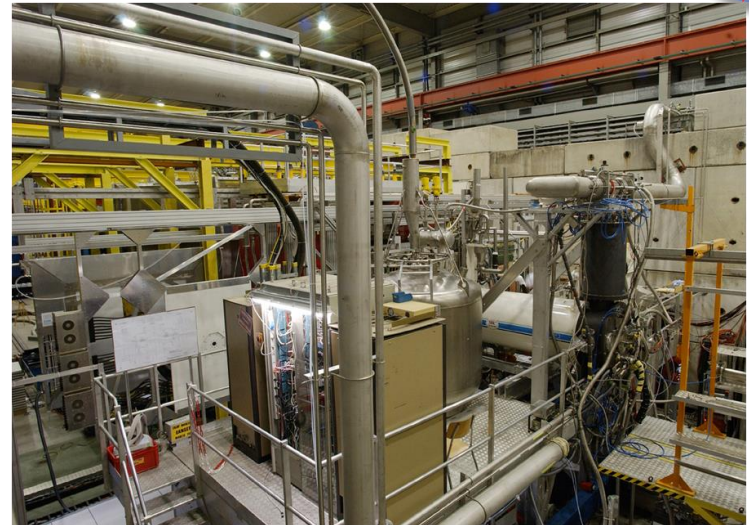
using a simple parametrisation we have calculated the
Confidence Levels from replicas



Hardware-wise the most "heavy" activity to be carried out is a COMPASS PT preparation.

Scenario of 2019 and 2020





- Jan 2019: Target platform movement
- Feb-April 2019: Target pipes/cables installation
HM04/HM05 position adjustment
PA03/PA05 refurbishment
- May 2019: DR removal, 3 cell modification
- June 2019: cavity test, DR reinstallation,
DC5 transport to clean area,
SciFi 4 reinstallation
- Aug-Sept. 2019: crane renovation
- Sep. 2019: repair loose wire DC5 Y2
- Oct. 2019: start RICH Wall refurbishment
- Dec. 2019: DC4 to clean area for repair





Summary



- Analysis are going on for all research lines: Spectroscopy, SIDIS, Drell-Yan and GPDs
- Preparations for 2021 are well on track



Thank you!



SPARES